Korean J. Chem. Eng., 40(1), 175-184 (2023)
DOI: 10.1007/s11814-022-1236-7

pISSN: 0256-1115
eISSN: 1975-7220

Construction of amphiphilic networks in blend membranes for CO_2 separation

Jiangnan Wang*, Xia Lv*, Lu Huang*, Long Li*, Xueqin Li*,†, and Jinli Zhang*,,†**

*School of Chemistry and Chemical Engineering/Key Laboratory for Green Processing of Chemical Engineering of Xinjiang Bingtuan, Shihezi University, Shihezi, Xinjiang, 832003, China
**Key Laboratory for Green Chemical Technology of Ministry of Education, School of Chemical Engineering and Technology, Tianjin University, Tianjin 300072, China
(*Received 8 April 2022 • Revised 2 July 2022 • Accepted 19 July 2022*)

Abstract−Blend membranes have attracted great attention because they can combine the advantages of different polymers. To investigate the effect of amphiphilic polymer on the separation performance of blend membranes, a series of blend membranes were designed and fabricated by blending an amphiphilic polymer of poly(3,4-ethylenedioxythiophene):polystyrene sulfonate (PEDOT:PSS) into poly(ether-block-amide) (Pebax) polymer for CO_2 separation. For the as-prepared Pebax/PEDOT:PSS blend membranes, the interconnected CO_2-philic networks were constructed by hydrophilic anionic chains of PSS^- for accelerating CO_2 transport. Meanwhile, non-CO_2-philic networks were constructed by the hydrophobic cationic chains of $PEDOT^+$, which distributed around the PSS^- chains to provide low friction diffusion for CO_2. Therefore, the amphiphilic polymer of PEDOT:PSS was an excellent material for improving CO_2 separation performance of blend membranes. The results showed that the Pebax/PEDOT:PSS blend membranes were endowed with excellent CO_2 separation performance. Pebax/PEDOT:PSS blend membrane demonstrated the optimal separation performance with a CO_2 permeability of 440.2±3.3 Barrer and a CO_2/CH_4 separation factor of 28±0.6. This study indicates that introducing the amphiphilic polymer into the blend membranes is an efficient strategy for gas separation.

Keywords: Pebax, Amphiphilic Polymer, PEDOT:PSS, Blend Membrane, CO_2 Separation

INTRODUCTION

As a clean energy source, natural gas has played an important role in the global green and low-carbon energy transition [1-4]. In 2020, the consumption of natural gas as primary energy increased by 6.9% year-on-year [5]. However, natural gas generally contains 10-40 mol% CO_2, which not only reduces the calorific value of natural gas but also corrodes equipment and pipelines [6-9]. At present, the most pressing issue is removing CO_2 from raw natural gas to obtain high-purity natural gas in the process of natural gas application process. Compared with traditional technologies, membrane technology has several advantages in cost and environment. They have the advantage of high energy efficiency, simple and reliable operation, modular design, and ease to scale up, and low energy consumption [10,11]. They do not require energy-intensive phase changes or potentially expensive adsorbents, and they are easy to handle solvents [12]. Therefore, membrane technology is one of the most promising CO_2 separation technologies because of its simple operation, high separation efficiency, and low energy consumption [13].

Polymers are commonly used for fabricating CO_2 separation membranes because polymeric membranes are (i) much cheaper than inorganic membranes, (ii) able to be easily fabricated into commercially viable hollow fibers or flat sheets, and (iii) easily scalable [14]. Solution-diffusion mechanism is a basic transport mechanism of polymeric gas separation membranes. It was assumed that there were no permanent pores in the membranes and specific interaction between CO_2 and the membrane. Generally speaking, the transport of gas has three steps through the membrane. First, the gas is absorbed on the surface of membranes at the upstream side. Secondly, the gas diffuses through the membranes. Finally, the gas is desorbed at the downstream side [3,14,15]. However, the increased permeability mainly results from the faster diffusion of gases through the large polymer chain spacing, which inevitably leads to decreased selectivity for membranes. Therefore, the high-permeability membranes have low selectivity in most cases, and vice versa [16,17]. Therefore, a long-standing challenge is that a trade-off effect exists between the CO_2 permeability and CO_2/CH_4 selectivity for polymeric membranes [18-21].

Many approaches, such as blending, cross-linking, and grafting, have been adopted to overcome the challenge. Wherein, polymeric blending is to combine different polymers with distinct physical, chemical, and mechanical properties to fabricate blend membranes. A combination of useful properties of each polymer can be obtained by polymeric blending without the tedious work. And polymeric blending has several advantages in fabricating blend membranes, such as simplicity, excellent reproducibility, and low fabrication cost [22-26]. Thus, the study of blend membranes has attracted the attention of researchers.

In recent years, studies have shown that sulfonated polymer networks can increase CO_2 uptake up to 13.5% during sorption tests [27]. The results imply that blend membranes containing sulfonic acid groups have the potential to efficiently separate CO_2 from CH_4. Some researchers have begun to pay attention to the investigation

†To whom correspondence should be addressed.
E-mail: lixueqin861003@163.com, zhangjinli@tju.edu.cn

of blend membranes containing sulfonic acid groups. Yong et al. [28] prepared blend membranes by introducing sulfonated polyphenylenesulfone (sPPSU) into polymers of intrinsic microporosity (PIM-1) to investigate CO_2 separation performance. The results showed that the CO_2/CH_4 selectivity of blend membranes increased, while the CO_2 permeability decreased.

The increase of CO_2/CH_4 selectivity was caused by the strong interaction between CO_2 and sulfonic acid groups, which rendered high affinity with CO_2. It was indicated that the introducing sulfonic acid groups into blend membranes was beneficial to improve CO_2/CH_4 selectivity. However, the interaction between sulfonic acid groups and polymer resulted in polymer chain packing, decreasing the CO_2 permeability of blend membranes. Many literatures have proved that hydrophobic groups of the polymeric membranes could provide low friction diffusion for CO_2 transport, thus increasing CO_2 permeability [29,30]. As a result, it was required to design blend membranes containing sulfonic acid groups and hydrophobic groups to simultaneously improve CO_2/CH_4 selectivity and CO_2 permeability.

The effect of amphiphilic materials has also been observed in some biological systems. The stenocara beetle living in the Namib desert utilizes a hydrophobic surface with a random array of hydrophilic bumps on its back to efficiently collect drinking water in the low moisture environments it inhabits. The philic domains render preferential adsorption to enhance penetrant solubility and decrease the energy barrier into the channel, while the non-philic domains work as fast transport pathways, imparting low friction diffusion [31,32].

Poly(3,4-ethylenedioxythiophene):polystyrene sulfonate (PEDOT:PSS) contains abundant hydrophilic sulfonic acid groups on PSS^- chains and hydrophobic thiophene groups on $PEDOT^+$ chains, and it is a kind of commercial amphiphilic polymer. The sulfonic acid groups on the PSS^- chains can form hydrogen bonding and have strong molecular interaction with CO_2 [33-37]. The sulfonic acid groups on the PSS^- chains interact strongly with CO_2 [38,39]. And the interconnected PSS^- chains can construct hydrophilic CO_2-philic networks, which have the potential to improve the CO_2/CH_4 selectivity of blend membranes. Meanwhile, the existence of $PEDOT^+$ chains is conducive to promoting the rapid diffusion of CO_2 due to the weak interaction between CO_2 and hydrophobic thiophene groups [40,41]. Therefore, the introduction of $PEDOT^+$ chains has potential to improve CO_2 permeability of blend membranes.

Moreover, the electrostatic interaction between $PEDOT^+$ chains and PSS^- chains can reduce the interaction between sulfonic acid groups and other polymer chains, avoiding the chain packing of blend membranes [42,43]. It is indicated that the introduced PEDOT:PSS is beneficial for improving CO_2 permeability of blend membranes. Therefore, the introduction of PEDOT:PSS is expected to simultaneously improve CO_2/CH_4 selectivity and CO_2 permeability of blend membranes.

Pebax® MH 1657, composed of 40% polyimide segments (PA) and 60% polyether segments (PEO) in which PA provide mechanical properties and PEO have affinity for CO_2 [44-46], is a common commercial membrane material. In this study, a series of Pebax/PEDOT:PSS blend membranes were fabricated by blending different content of PEDOT:PSS with Pebax® MH 1657 (Pebax). The physicochemical properties of the Pebax/PEDOT:PSS blend membranes were characterized and analyzed. Finally, the effect of PEDOT:PSS loading on the CO_2 separation performance of the blend membrane was tested, and the effect of feed pressure on the CO_2 separation performance was tested and discussed.

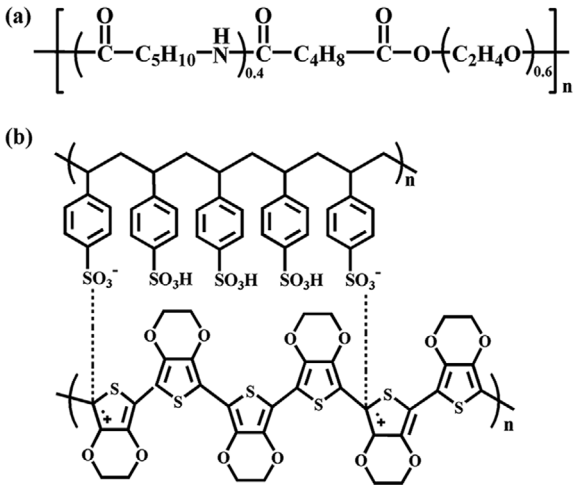

Fig. 1. Chemical structure of (a) Pebax, (b) PEDOT:PSS.

MATERIALS AND METHODS

1. Materials

Pebax® MH 1657 (Pebax, Fig. 1(a)) was purchased from Shanghai Rongtian Chemical Co. Ltd. Pebax 1657 is a polyether-block-amide comprising 40% polyimide segments (PA, nylon-6) and 60% polyether segments (PEO). The block size of the PEO segment is around 1,500 g/mol, which means that one repeating unit (n) consists of a PEO-block containing approximately 35 ethylene oxide units and a PA-block containing approximately 9 nylon-6 repeating units. The molecular weight (Mw) of Pebax 1657 is between 30,000 and 50,000 $g \cdot mol^{-1}$ [47,48]. Poly(3,4-ethylenedioxythiophene):polystyrene sulfonate (PEDOT:PSS, 1.4% in water, Fig. 1(b), viscosity: 30 mPa·s, solid content: 1.71%) and ethanol were purchased from Adamas Corporation. Deionized water was made in our laboratory.

2. Membrane Preparation

The membranes were prepared by the solvent casting method. However, the amide block was difficult to dissolve into the common organic solvents [49]. The research proved the stable Pebax solution was easily obtained by dissolving Pebax in a mixture 70% ethanol/30% water with reflux at 80 °C [39,50,51]. Therefore, a specific amount of Pebax was added into 70% ethanol solution and then stirred at 80 °C for 2 h to completely dissolve. After cooling for half an hour, 6 wt% Pebax solutions were obtained. A certain amount of PEDOT:PSS was added into the Pebax solution prepared above and stirred for 4 h at 25 °C until the PEDOT:PSS was evenly mixed in the solution to obtain the casting solution. The obtained casting solution was poured onto a flat glass plate for tape casting and dried at 25 °C for 48 h and then put into a 40 °C vacuum oven to remove the residual solvent to obtain Pebax/PEDOT:PSS blend membranes.

Pure Pebax membranes were also fabricated according to the

above method without PEDOT:PSS loading. For simplicity, the obtained membranes were designated as Pebax/PEDOT:PSS-*X*, where *X* was in a range of 3-9 wt%, referring to the weight percentage of loading (PEDOT:PSS) relative to the weight of Pebax. The membrane thickness was about 100-120 μm.

The PEDOT:PSS loadings are defined as Eq. (1)

$$X_{PEDOT:PSS}=\frac{m_{PEDOT:PSS}}{m_{PEDOT:PSS}+m_{Pebax}}\times 100\% \quad (1)$$

where the units of $m_{PEDOT:PSS}$ and m_{Pebax} is g.

3. Membrane Characterization

The cross-sectional images of pure Pebax membrane and Pebax/PEDOT:PSS blend membranes were investigated by using a scanning electron microscope (SEM, JSM-6490 LV). X-Ray diffraction (XRD, Bruker D8 ADVANCE) was used to investigate the crystalline structure of pure Pebax membrane and Pebax/PEDOT:PSS blend membranes. The presence of functional groups in the fabricated Pebax/PEDOT:PSS blend membranes was recorded by attenuated total reflection Fourier transform infrared spectroscopy (ATR-FTIR, BRUKER Vertex 70). The CO_2 adsorption isotherms were tested by ASAP 2460 analyzer in the 0-100 kPa range at 298 K. The hydrophilicity of the membrane was tested with deionized water, and the contact angle of the membrane was obtained. The mechanical properties of pure Pebax membrane and the blend membranes were tested by the tensile strength test.

4. Gas Permeation Measurement

In this study, gas separation performance was reflected by the permeability and selectivity of CO_2 or CH_4. The separation performance of the pure Pebax membrane and blend membranes was tested by using a binary mixture gas system (CO_2/CH_4=20/80 vol%) under humidified conditions with the feed and sweep gas fluxes of 50 and 30 mL/min, respectively [52]. A self-made test device was used for gas penetration test; the test temperature was 25 °C and the pressure range was 28 bar [53]. Under humidified conditions, a schematic diagram of gas separation device for CO_2/CH_4 separation is shown in Fig. 2. The effective membrane area was 12.56 cm^2. Gas composition was analyzed using Shimadzu GC2014C gas chromatograph.

The permeability of the gas component can be calculated by Eq. (2):

$$P_i=\frac{Q_i l}{\Delta P_i A} \quad (2)$$

where P_i is the CO_2 and CH_4 permeability (Barrer, 1 Barrer=10^{-10} cm^3 (STP) cm/cm^2 s cmHg), Q_i is the volumetric flow of gas (cm^3 (STP)/s), l is the thickness of the membrane (cm), ΔP_i (cmHg) is the partial pressure difference between two sides of the membrane of gas i, and A is the permeation area of the membrane.

The selectivity of the gas component can be calculated by Eq. (3):

$$\alpha_{ij}=\frac{P_i}{P_j} \quad (3)$$

P_i and P_j are the permeability coefficients of component i and component j, respectively. When the feed gas is pure, α_{ij} is the ideal selectivity of i/j component. When the feed gas is a mixture, α_{ij} is the separation factor of i/j component.

RESULTS AND DISCUSSION

1. Characterization of Pebax/PEDOT:PSS Blend Membrane

1-1. SEM

The cross-sectional morphologies of pure Pebax membrane and Pebax/PEDOT:PSS blend membranes are clearly observed from SEM images in Fig. 3. Fig. 3(a) demonstrates that the cross-section of the pure Pebax membrane was smooth and free of imperfection. It is shown that the cross-sectional morphology of Pebax/PEDOT:PSS blend membranes did not change much with the increased PEDOT:PSS loading in Fig. 3(b)-(e). In addition, no voids were observed in the cross-sections of the Pebax/PEDOT:PSS blend membranes. This indicates that the amphiphilic polymer of PEDOT:PSS had good compatibility with Pebax polymer in the blend mem-

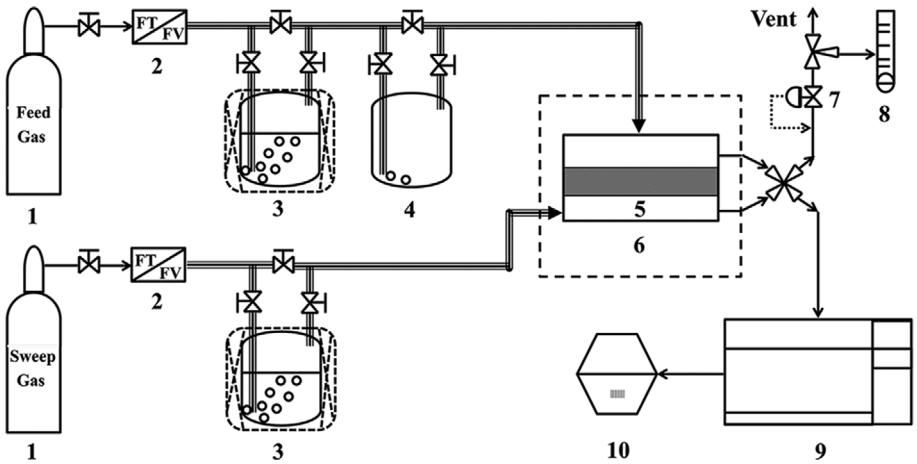

Fig. 2. Schematic diagram of humidified test device.

1. Gas cylinder
2. Mass flow meter
3. Humidifier with heating belts
4. Water knockout
5. Membrane cell
6. Oven
7. Back pressure regulator
8. Soap film flowmeter
9 Gas chromatography
10. Computer

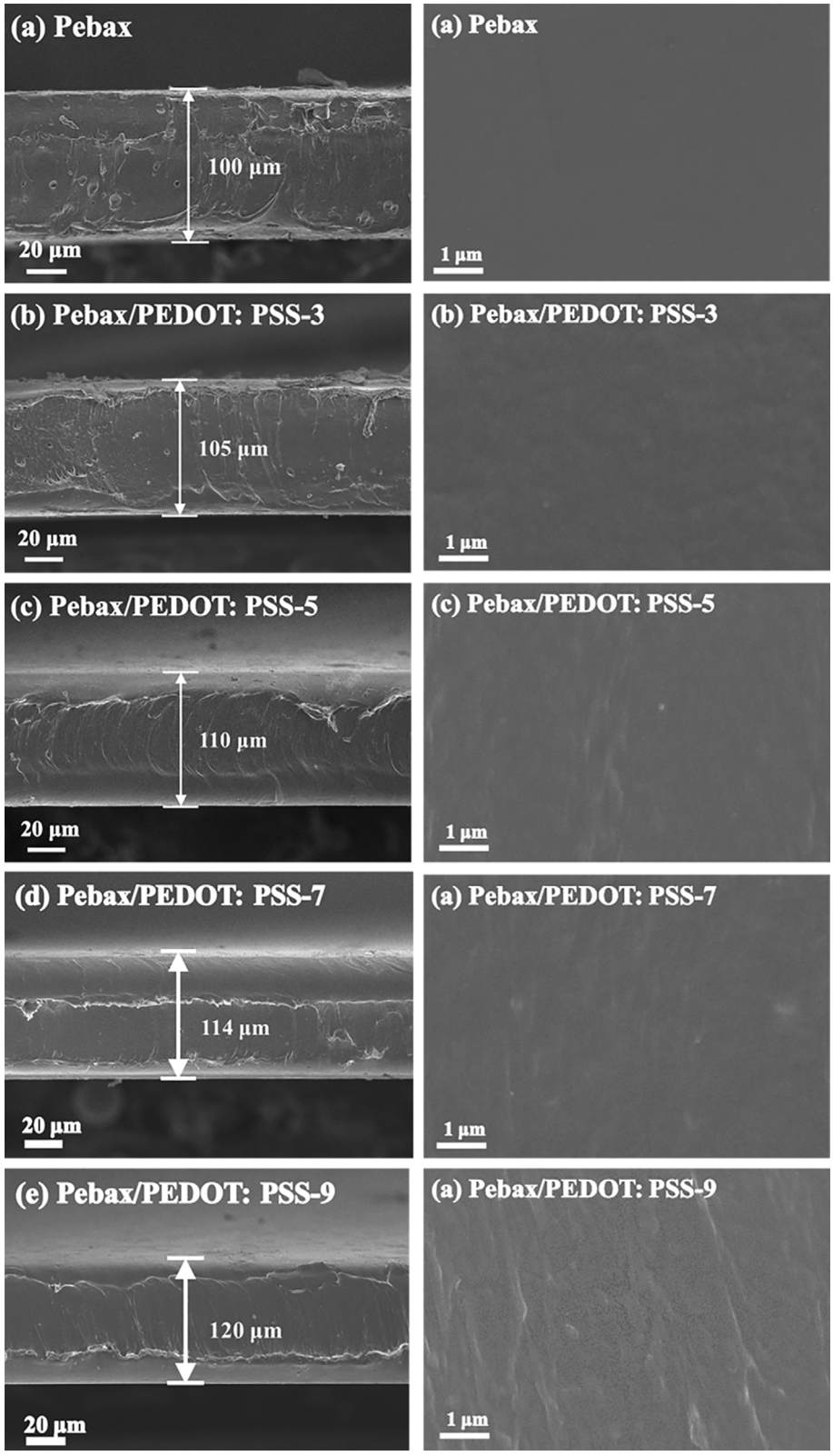

Fig. 3. SEM images of cross-section of membranes.

branes.

The elemental distribution of the pure Pebax membrane and Pebax/PEDOT:PSS blend membrane was confirmed by the elemental mapping images; the results are shown in Fig. 4. It is shown that the C, O, and N atoms are uniformly distributed in all membranes. And a uniform distribution of S atoms is observed in Pebax/

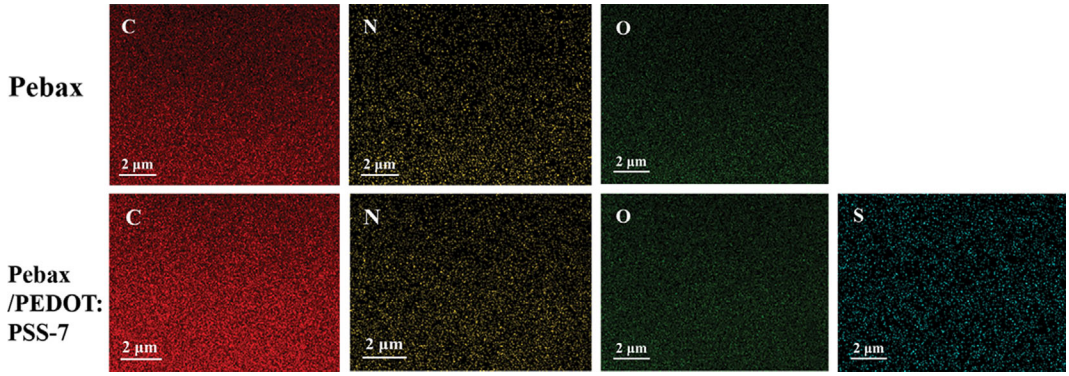

Fig. 4. Elemental mapping images of membranes.

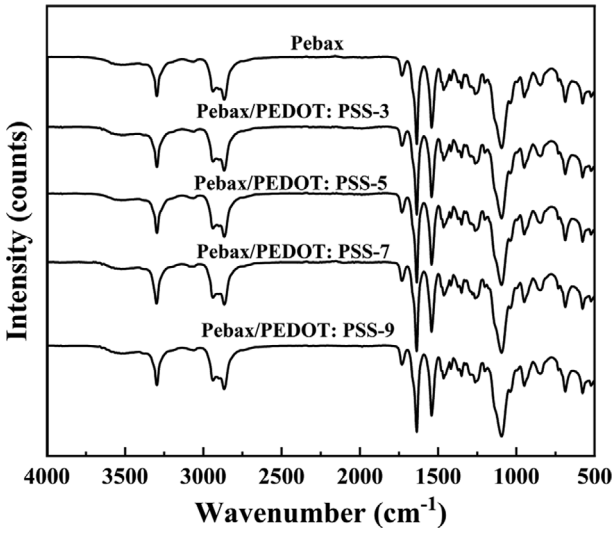

Fig. 5. ATR-FTIR spectra of pure Pebax membrane and Pebax/PEDOT:PSS blend membranes.

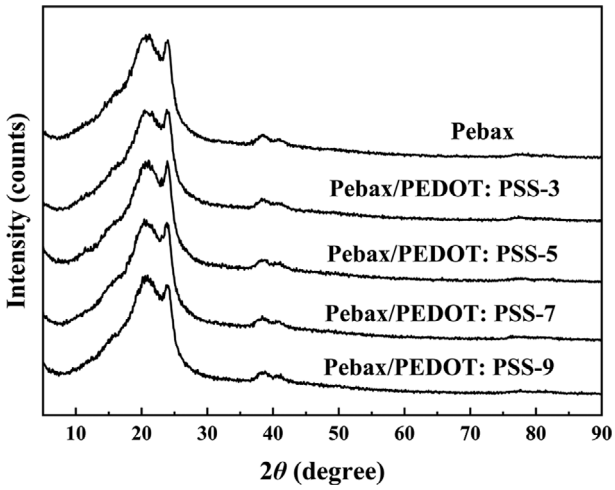

Fig. 6. XRD patterns of pure Pebax membrane and Pebax/PEDOT:PSS blend membranes.

PEDOT:PSS blend membrane by introducing PEDOT:PSS into Pebax. It indicates that PEDOT:PSS was successfully introduced in blend membranes.

1-2. ATR-FTIR

The ATR-FTIR spectra of pure Pebax membrane and Pebax/PEDOT:PSS blend membranes are presented in Fig. 5. In the spectrum of pure Pebax membrane, the infrared characteristic peaks located at 3,297 cm^{-1} and 1,636 cm^{-1} correspond to the stretching vibrations of the N-H bond and the H-N-C=O bond, respectively. The infrared characteristic peaks located at 1,730 cm^{-1} and 1,096 cm^{-1} correspond to the stretching vibrations of the C=O bond and the C-O-C bond, respectively. These results are consistent with the molecular structure formula of Pebax 1657 [52,54].

The pure Pebax membrane and the Pebax/PEDOT:PSS blend membranes had similar characteristic peaks as shown in Fig. 5. In Fig. 5, no new peak appeared in the spectra of blend membranes in comparison with that of the pure membrane, and the changes of the characteristic bands were not clearly observed in Pebax/PEDOT:PSS blend membranes. It was mainly attributed to the fact that PEDOT:PSS had good compatibility with Pebax and no effect on the chemical structure of Pebax.

1-3. XRD

The XRD patterns of pure Pebax membrane and Pebax/PEDOT:PSS blend membranes are presented in Fig. 6. The crystal structure and molecular-chain spacing of the membranes were analyzed. It was demonstrated that the broad peaks ranging from 15° to 30° were characteristic diffraction peaks of crystalline polyamide (PA6) phase and amorphous polyethylene oxide (PEO) phase in Pebax 1657 [55].

The average *d*-spacings of pure Pebax membrane and Pebax/PEDOT:PSS blend membranes were calculated according to Bragg's law [56]. At the sharp peak 2θ=24°, the pure Pebax membrane showed a *d*-spacing of 0.379 nm, and the Pebax/PEDOT:PSS blend membranes showed larger *d*-spacings in comparison with that of pure Pebax membrane. The Pebax/PEDOT:PSS-7 blend membrane showed the greatest *d*-spacing of 0.383 nm at the sharp peak 2θ=23.7°. The possible reason for this change was that the interaction between PEDOT:PSS and Pebax could have disrupted the original Pebax chain packing, particularly the crystalline PA region [39]. The increased *d*-spacings could improve the CO_2 permeability of the blend membrane. The results implied that the introduction of PEDOT:PSS was beneficial to increase the CO_2 permeability of the blend membrane.

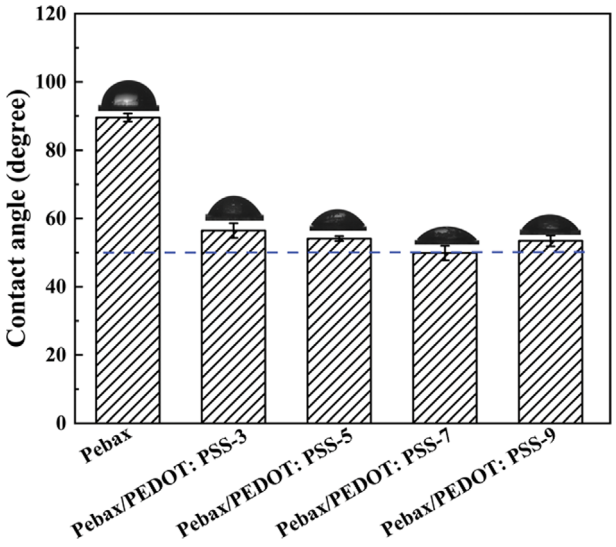

Fig. 7. The histogram of contact angle of pure membrane and Pebax/PEDOT:PSS blend membranes.

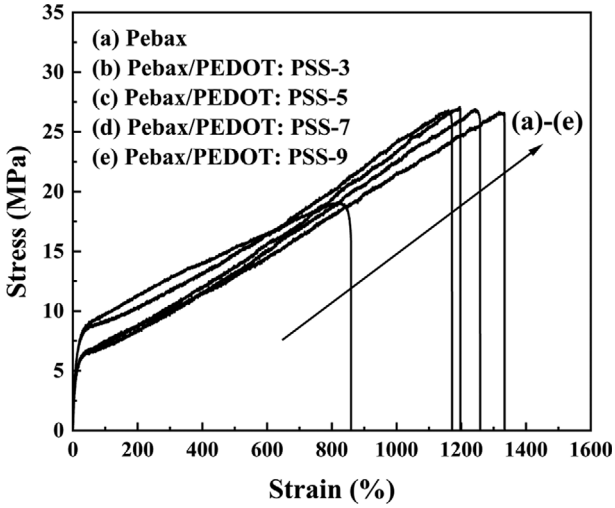

Fig. 8. The stress-strain curves of pure Pebax membrane and the blend membranes.

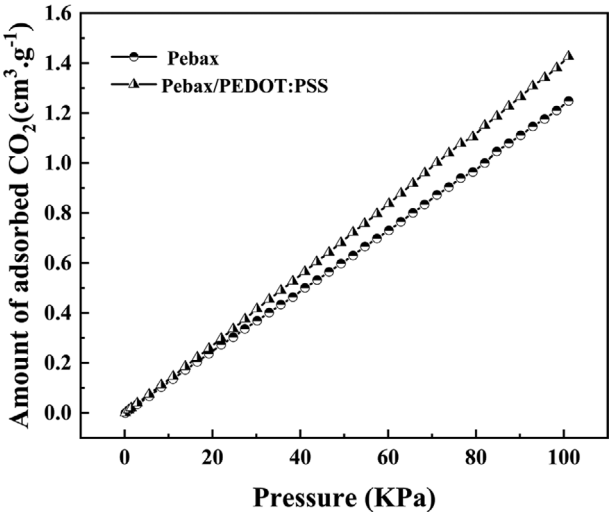

Fig. 9. The CO_2 adsorption isotherms of membranes

1-4. Contact Angle

The contact angle histogram of pure membrane and Pebax/PEDOT:PSS blend membranes is presented in Fig. 7. It is shown that the contact angle of pure Pebax membrane was 89.5°. And the contact angles of the Pebax/PEDOT:PSS blend membranes continued to decrease when the PEDOT:PSS loading was less than 7 wt%. The main reason for the decrease is that the PSS^- chains in PEDOT:PSS contained plentiful hydrophilic $-SO_3^-$ anions and $-SO_3H$ groups. These units and groups endowed PEDOT:PSS with hydrophilicity and absorbed water molecules that selectively promoted CO_2 transport [57,58]. It suggested that the introduced PEDOT:PSS could be beneficial for improving the CO_2 separation performance of the Pebax/PEDOT:PSS blend membranes. However, the contact angles became slightly increased when the PEDOT:PSS loadings were increased from 7 wt% to 9 wt%. This might arise from the agglomeration of $PEDOT^+$ chains and PSS^- chains, which resulted in a decrease in hydrophilic regions.

1-5. Mechanical Properties

The mechanical properties of pure membrane and the blend membranes are shown in Table 1 and Fig. 8. It is seen from Table 1 that Young's modulus of the blend membranes increased after adding PEDOT:PSS. It resulted from the interaction between PEDOT:PSS and PEO segments in Pebax [42]. In addition, the mechanical properties of the blend membranes improved by the introduction of PEDOT:PSS. It is attributed to the amphiphilic network structures formed between $PEDOT^+$ segment and PSS^- segment in the blend membrane [59-61].

1-6. CO_2 Adsorption Capacity

The CO_2 adsorption isotherms of the pure Pebax membrane and Pebax/PEDOT:PSS-7 blend membrane at 298 K are displayed

Table 1. Mechanical properties of membranes

Membrane	Elongation at break (%)	Tensile strength (MPa)	Young's modulus (MPa)
Pebax	865.90±21.4	19.10±1.1	30.05±2.1
Pebax/PEDOT:PSS-3	1,176.91±22.3	26.82±1.9	40.79±1.3
Pebax/PEDOT:PSS-5	1,263.45±28.1	26.91±1.7	58.39±1.9
Pebax/PEDOT:PSS-7	1,339.12±16.5	26.68±2.1	60.27±2.3
Pebax/PEDOT:PSS-9	1,203.60±19.7	27.08±1.5	78.79±1.6

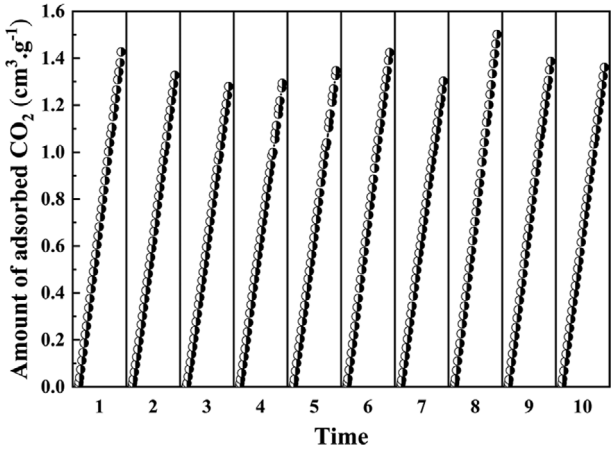

Fig. 10. The CO_2 adsorption capacity of the Pebax/PEDOT:PSS-7 blend membrane through ten adsorption/desorption cycles.

in Fig. 9. It is shown that CO_2 adsorption capacity increased with increasing pressure. The Pebax/PEDOT:PSS-7 blend membrane exhibited higher CO_2 adsorption capacity than the pure Pebax membrane, highlighting its excellent affinity for CO_2. It resulted from the rich CO_2-philic groups (sulfonic acid groups and benzene rings) in PEDOT:PSS. And it implied that the introduction of PEDOT:PSS was beneficial for increasing the CO_2/CH_4 selectivity of blend membranes.

To test the recyclability of CO_2 adsorption capacity, the CO_2 adsorption capacity of the blend membrane was measured through ten adsorption/desorption cycles at 298 K, and the results are shown in Fig. 10. The adsorbed CO_2 was removed by dynamic vacuum treatment at 80 °C for 2 h between each cycle. The results showed that the absorption capacity remained basically unchanged through ten adsorption/desorption cycles, indicating that the Pebax/PEDOT:PSS blend membrane had excellent recyclability.

2. Gas Separation Performance

2-1. Mixed-gas

To simulate the separation performance of Pebax/PEDOT:PSS blend membranes under real conditions, the separation performance

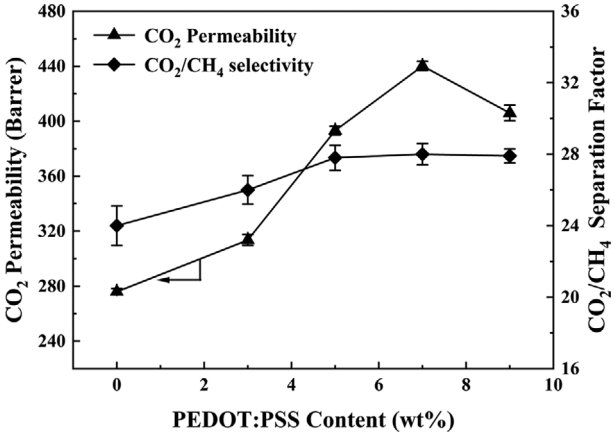

Fig. 11. CO_2/CH_4 separation performance of the Pebax membrane and Pebax/PEDOT:PSS blend membranes under humidified conditions.

of pure Pebax membrane and Pebax/PEDOT:PSS blend membranes with different loadings was tested under humidified conditions. The CO_2 permeability and CO_2/CH_4 separation factors of the blend membranes are shown in Fig. 11.

It is shown that the CO_2 permeability and CO_2/CH_4 separation factors of Pebax/PEDOT:PSS blend membranes were found to be superior to that of the pure membrane. And CO_2 permeability and CO_2/CH_4 separation factors increased first, and then decreased as the PEDOT:PSS loadings increased from 3 wt% to 9 wt% as for Pebax/PEDOT:PSS blend membranes. The CO_2 permeability and CO_2/CH_4 separation factor of Pebax/PEDOT:PSS blend membrane reached the highest (P_{CO2}=440.2±3.3 Barrer, $\alpha_{CO2/CH4}$=28±0.6) at the PEDOT:PSS loading of 7 wt%, increasing by 60% and 17%, respectively, in comparison to that of pure Pebax membrane.

The enhancement of CO_2 separation performance was primarily due to the CO_2-philic/non-CO_2-philic network structures and high-CO_2-philic groups of PEDOT:PSS [62]. On one hand, since there were plenty of hydrophilic groups on the anionic chain of PSS^-, the interconnected CO_2-philic network structures were constructed by the introduced amphiphilic polymer of PEDOT:PSS in the blend membranes [63]. The interconnected CO_2-philic networks were beneficial for facilitating the absorbed water molecules that selectively promoted CO_2 transport [64-66]. Meanwhile, the hydrophobic cationic chains of $PEDOT^+$ constructed the non-CO_2-philic networks, thus rendering the low-friction fast diffusion of CO_2 [40,41]. The interlaced hydrophobic and hydrophilic chains were beneficial for accelerating fast CO_2 transport and diffusion, thus improving the CO_2 permeability and CO_2/CH_4 separation factor.

On the other hand, sulfonic acid groups and benzene rings on PSS^- chains in PEDOT:PSS had strong interactions with CO_2. These interactions include: (1) The hydrogen bonding interaction between SO_3H and CO_2; (2) The electrostatic interaction between RSO_3^- and CO_2; and (3) The quadrupole-π interaction between benzene rings and CO_2 [38,39]. In addition, CO_2 and sulfonated ligands were hard Lewis acid and hard bases, respectively. According to Pearson's Hard-soft acid-base (HSAB) principle [67,68], CO_2 (hard acid) takes precedence over sulfonate groups (hard base) in the formation of stable complexes. Therefore, the Pebax/PEDOT:PSS blend membranes had an efficient effect on the CO_2/CH_4 separation because of the CO_2-philic/non-CO_2-philic network structure and high-CO_2-philic groups.

2-2. Effect of Feed Pressure

The effect of different feed pressure on the CO_2 separation performance of pure Pebax membrane and Pebax/PEDOT:PSS blend membranes was investigated, and the results are shown in Fig. 12. When the feed pressure was increased from 2 bar to 8 bar, the CO_2 permeability and CO_2/CH_4 separation factors of the pure Pebax membrane decreased by 48% and 26%, respectively. The decrease was mainly because the strongly polarizable CO_2 had a compression effect on mobile Pebax polymer chains, thus leading to the decrease of CO_2/CH_4 separation factors and CO_2 permeability. For the Pebax/PEDOT:PSS blend membranes, with the increase of the feed pressure, the CO_2 permeability and CO_2/CH_4 separation factors decreased by 34% and 19%, respectively, significantly lower than that of pure Pebax membrane. This is because the introduced PEDOT:PSS disrupted the arrangement of the original Pebax chain

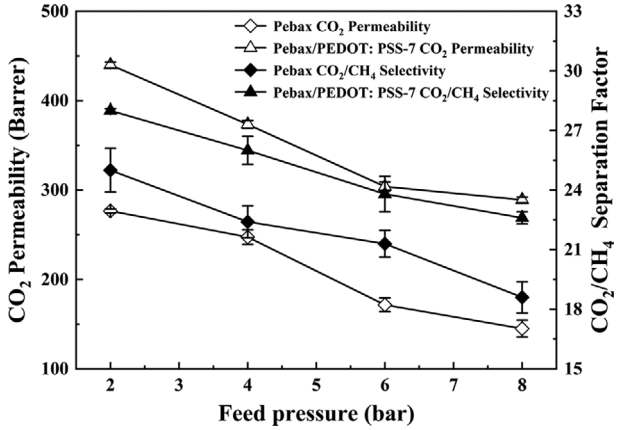

Fig. 12. Effect of feed pressure on CO_2 permeability and CO_2/CH_4 selectivity of the membranes.

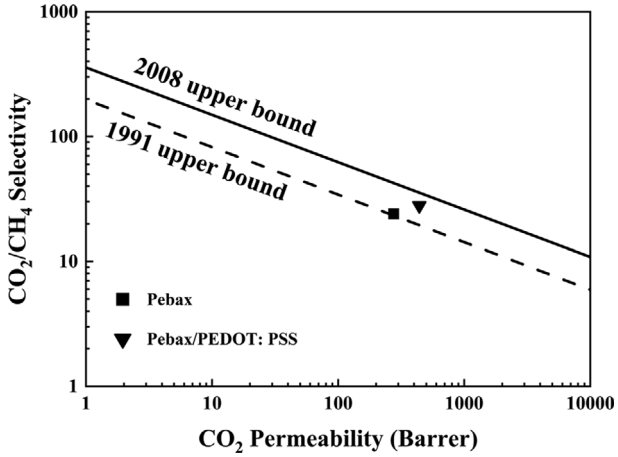

Fig. 13. Comparison of CO_2 separation performance of membranes with Robeson's upper bound.

and restricted the movement of polymer chains [69]. As a result, Pebax/PEDOT:PSS blend membranes were less affected by the high feed pressure than the pure membrane, thus improving CO_2 separation performance of Pebax/PEDOT:PSS blend membranes.

3. Comparison with Pebax-based Blend Membranes

Fig. 13 shows the CO_2 separation performance of the membranes in the upper bound limit plot [70]. Table 2 lists the CO_2 separation performance of existing Pebax-based blend membranes. It can be seen in Fig. 13 that the separation performance of the Pebax/PEDOT:PSS-7 blend membrane was close to the Robeson upper bound 2008. And it was demonstrated that the CO_2 separation performance of Pebax/PEDOT:PSS-7 blend membranes was higher than that of other Pebax-based blend membranes. It was mainly attributed to the fact that the co-existence of CO_2-philic networks and non-CO_2-philic networks contributed to the fast CO_2 transport and diffusion, resulting in improving CO_2 separation performance. The results suggest that the strategy of introducing amphiphilic polymer of PEDOT:PSS into Pebax polymer appears to be efficient in improving CO_2 separation performance of blend membranes.

CONCLUSIONS

Blend membranes were fabricated by blending poly (3,4-ethylenedioxythiophene):polystyrene sulfonate (PEDOT:PSS) with poly(ether-block-amide) (Pebax) for efficient CO_2 separation. PEDOT:PSS played a vital role in improving CO_2 separation performance of blend membranes. CO_2-philic networks and non-CO_2-philic networks were constructed by the hydrophilic chains of PSS^- and the hydrophobic chains of $PEDOT^+$, respectively. The co-existence of CO_2-philic networks and non-CO_2-philic networks contributed to the fast CO_2 transport, resulting in improving CO_2 separation performance. At 7 wt% loading, the blend membrane showed that the optimal gas separation performance was close to the 2008 Robson's upper bound. Though it is a challenge to explore the new Pebax-based blend membranes with high separation performance, blending Pebax with amphiphilic polymer can effectively improve separation performance by constructing amphiphilic networks in blend membranes. Therefore, it is necessary to explore amphiphilic polymers that can be blended with Pebax to obtain the high-performance blend membrane in the future.

ACKNOWLEDGEMENTS

This work was supported by the National Natural Science Foundation for Young Scientists of China [grant number 21706166]; the Program for Young and Middle-aged Scientific and Technological Innovation Leaders in Bingtuan [grant number 2019CB024]; the Program for Young Innovative Talents of Shihezi University [grant numbers CXRC201802]; and the Major Science and Technology Project of Xinjiang Bingtuan [grant number 2017AA007/01]. We wish to thank the Analysis and Testing Center of Shihezi University for the microscopy and microanalysis of our specimens.

Table 2. Comparison of separation performances of blend membranes fabricated in this work with other Pebax-based blend membranes

Membrane types -material	Loading (wt%)	Test condition	Test gas	Test state	P (CO_2)	α (CO_2/CH_4)	Ref.
Pebax 1657/PEG600	20	25 °C 7 bar	Pure gas	Dry	72.39	19	[71]
Pebax 1657/ PEG-ran-PPG	50	30 °C 3 bar	Pure gas	Dry	677	15.7	[72]
Pebax 1657/([BMIM][BF_4]	50	35 °C 10 bar	Pure gas	Dry	190	24.4	[73]
Pebax 1657/[Omim][PF_6]	8	30 °C 10 bar	Pure gas	Dry	185.3	19.7	[74]
Pebax 1657/PEGDME/[P_{66614}] [2-Op]	-	25 °C 0.3 bar	Pure gas	Dry	672.1	17.7	[71]
Pebax 1657/P(VAc-co-DBM)	30	25 °C 3 bar	Pure gas	Dry	103	37.5	[75]
Pebax 1657/PEDOT:PSS	8	25 °C 2 bar	Mixed gas	Wet	440.2	28	This study

REFERENCES

1. Q. Hou, Y. Wu, S. Zhou, Y. Wei, J. Caro and H. Wang, *Angew. Chem. Int. Ed.*, **58**, 327 (2019).
2. X. Li, J. Hou, R. Guo, Z. Wang and J. Zhang, *ACS Appl. Mater. Interfaces*, **11**, 24618 (2019).
3. B. Wang, M. Sheng, J. Xu, S. Zhao, J. Wang and Z. Wang, *Small Methods*, **4**, 1900749 (2020).
4. S. Wang, X. Li, H. Wu, Z. Tian, Q. Xin, G. He, D. Peng, S. Chen, Y. Yin, Z. Jiang and M. D. Guiver, *Energy Environ. Sci.*, **9**, 1863 (2016).
5. Y. Xin, K. Wang, Y. Zhang, F. Zeng, X. He, S. A. Takyi and P. Tontiwachwuthikul, *Energies*, **14**, 6883 (2021).
6. A. Raza, M. Askari, C. Z. Liang, N. Peng, S. Farrukh, A. Hussain and T.-S. Chung, *J. Membr. Sci.*, **625**, 119124 (2021).
7. Q. Qian, P. A. Asinger, M. J. Lee, G. Han, K. Mizrahi Rodriguez, S. Lin, F. M. Benedetti, A. X. Wu, W. S. Chi and Z. P. Smith, *Chem. Rev.*, **120**, 8161 (2020).
8. X. Lv, L. Huang, S. Ding, J. Wang, L. Li, C. Liang and X. Li, *Sep. Purif. Technol.*, **276**, 119347 (2021).
9. F. M. Baena-Moreno, E. le Saché, L. Pastor-Pérez and T. R. Reina, *Environ. Chem. Lett.*, **18**, 1649 (2020).
10. S. Basu, A. L. Khan, A. Cano-Odena, C. Liu and I. F. Vankelecom, *Chem. Soc. Rev.*, **39**, 750 (2010).
11. P. Bernardo and E. Drioli, *Pet. Chem.*, **50**, 271 (2010).
12. M. Rezakazemi, A. Ebadi Amooghin, M. M. Montazer-Rahmati, A. F. Ismail and T. Matsuura, *Prog. Polym. Sci.*, **39**, 817 (2014).
13. H. Wang, M. Wang, X. Liang, J. Yuan, H. Yang, S. Wang, Y. Ren, H. Wu, F. Pan and Z. Jiang, *Chem. Soc. Rev.*, **50**, 5468 (2021).
14. S. Wang, X. Li, H. Wu, Z. Tian, Q. Xin, G. He, D. Peng, S. Chen, Y. Yin, Z. Jiang and M. D. Guiver, *Energy Environ. Sci.*, **9**, 1863 (2016).
15. C. Ma, M. Wang, Z. Wang, M. Gao and J. Wang, *J. CO_2 Util.*, **42**, 101296 (2020).
16. C. Y. Chuah, K. Goh, Y. Yang, H. Gong, W. Li, H. E. Karahan, M. D. Guiver, R. Wang and T. H. Bae, *Chem. Rev.*, **118**, 8655 (2018).
17. Y. Han and W. S. W. Ho, *J. Membr. Sci.*, **628**, 119244 (2021).
18. Y. Zhang, J. Sunarso, S. Liu and R. Wang, *Int. J. Greenhouse Gas Control*, **12**, 84 (2013).
19. M. Sarfraz and M. Ba-Shammakh, *J. Taiwan Inst. Chem. Eng.*, **65**, 427 (2016).
20. N. Du, H. B. Park, M. M. Dal-Cin and M. D. Guiver, *Energy Environ. Sci.*, **5**, 7306 (2012).
21. B. Comesaña-Gándara, J. Chen, C. G. Bezzu, M. Carta, I. Rose, M.-C. Ferrari, E. Esposito, A. Fuoco, J. C. Jansen and N. B. McKeown, *Energy Environ. Sci.*, **12**, 2733 (2019).
22. P. Taheri, A. Raisi and M. S. Maleh, *Environ. Sci. Pollut. Res.*, **28**, 38274 (2021).
23. K. K. Wong and Z. A. Jawad, *J. Polym. Res.*, **26**, 289 (2019).
24. R. Xing and W. S. W. Ho, *J. Taiwan Inst. Chem. Eng.*, **40**, 654 (2009).
25. W. F. Yong, F. Y. Li, Y. C. Xiao, P. Li, K. P. Pramoda, Y. W. Tong and T. S. Chung, *J. Membr. Sci.*, **407-408**, 47 (2012).
26. W. F. Yong and H. Zhang, *Prog. Mater. Sci.*, **116**, 100713 (2021).
27. W. Lu, D. Yuan, J. Sculley, D. Zhao, R. Krishna and H. C. Zhou, *J. Am. Chem. Soc.*, **133**, 18126 (2011).
28. W. F. Yong, Z. K. Lee, T. S. Chung, M. Weber, C. Staudt and C. Maletzko, *ChemSusChem*, **9**, 1953 (2016).
29. Q. Gou, H. Luo, Y. Zheng, Q. Zhang, C. Li, J. Wang, O. Odunmbaku, J. Zheng, J. Xue, K. Sun and M. Li, *Small*, **18**, e2201732 (2022).
30. Y. Liu, Z. Wang, M. Shi, N. Li, S. Zhao and J. Wang, *Chem. Commun.*, **54**, 7239 (2018).
31. L. Wang, C. Yang, B. Zhao, X. Wu, Z. Yu, L. Zhao, H. Zhang and N. Li, *J. Membr. Sci.*, **569**, 157 (2019).
32. S. Wang, Y. Xie, G. He, Q. Xin, J. Zhang, L. Yang, Y. Li, H. Wu, Y. Zhang, M. D. Guiver and Z. Jiang, *Angew. Chem. Int. Ed.*, **56**, 14246 (2017).
33. M. Berggren, X. Crispin, S. Fabiano, M. P. Jonsson, D. T. Simon, E. Stavrinidou, K. Tybrandt and I. Zozoulenko, *Adv. Mater.*, **31**, 1805813 (2019).
34. Y. Honma, K. Itoh, H. Masunaga, A. Fujiwara, T. Nishizaki, S. Iguchi and T. Sasaki, *Adv. Electron. Mater.*, **4**, 1700490 (2018).
35. M. Modarresi, A. Mehandzhiyski, M. Fahlman, K. Tybrandt and I. Zozoulenko, *Macromolecules*, **53**, 6267 (2020).
36. A. V. Volkov, K. Wijeratne, E. Mitraka, U. Ail, D. Zhao, K. Tybrandt, J. W. Andreasen, M. Berggren, X. Crispin and I. V. Zozoulenko, *Adv. Funct. Mater.*, **27**, 1700329 (2017).
37. Y. Yang, G. Zhao, X. Cheng, H. Deng and Q. Fu, *ACS Appl. Mater. Interfaces*, **13**, 14599 (2021).
38. A. Torrisi, C. Mellot-Draznieks and R. G. Bell, *J. Chem. Phys.*, **132**, 044705 (2010).
39. N. Zhang, D. Peng, H. Wu, Y. Ren, L. Yang, X. Wu, Y. Wu, Z. Qu, Z. Jiang and X. Cao, *J. Membr. Sci.*, **549**, 670 (2018).
40. W. Liang, Y. Chenyang, Z. Bin, W. Xiaona, Y. Zijun, Z. Lixiang, Z. Hongwei and L. Nanwen, *J. Membr. Sci.*, **569**, 157 (2019).
41. R. U. Rehman, Q. Song, L. Peng, Y. Chen and X. Gu, *Chin. J. Chem. Eng.*, **27**, 2397 (2019).
42. P. Li, K. Sun and J. Ouyang, *ACS Appl. Mater. Interfaces*, **7**, 18415 (2015).
43. J. H. Lee, J. P. Jung, E. Jang, K. B. Lee, Y. J. Hwang, B. K. Min and J. H. Kim, *J. Membr. Sci.*, **518**, 21 (2016).
44. J. Cheng, Y. Wang, L. Hu, N. Liu, J. Xu and J. Zhou, *J. Membr. Sci.*, **597**, 117644 (2020).
45. A. Ioannidi, D. Vroulias, J. Kallitsis, T. Ioannides and V. Deimede, *J. Membr. Sci.*, **632**, 119353 (2021).
46. B. Zhu, X. Jiang, S. He, X. Yang, J. Long, Y. Zhang and L. Shao, *J. Mater. Chem. A*, **8**, 24233 (2020).
47. J. Didden, R. Thür, A. Volodin and I. F. J. Vankelecom, *J. Appl. Polym. Sci.*, **135**, 46433 (2018).
48. S. R. Reijerkerk, M. H. Knoef, K. Nijmeijer and M. Wessling, *J. Membr. Sci.*, **352**, 126 (2010).
49. J. H. Kim, S. Y. Ha and Y. M. Lee, *J. Membr. Sci.*, **190**, 179 (2001).
50. R. He, S. Cong, S. Xu, S. Han, H. Guo, Z. Liang, J. Wang and Y. Zhang, *J. Membr. Sci.*, **624**, 119081 (2021).
51. Q. Zhang, M. Zhou, X. Liu and B. Zhang, *J. Membr. Sci.*, **636**, 119612 (2021).
52. S. Ding, X. Li, S. Ding, W. Zhang, R. Guo and J. Zhang, *Sep. Purif. Technol.*, **239**, 116539 (2020).
53. Y. Wang, N. Zhang, H. Wu, Y. Ren, L. Yang, X. Wang, Y. Wu, Y. Liu, R. Zhao and Z. Jiang, *J. Membr. Sci.*, **618**, 118691 (2021).
54. H. Zhang, R. Guo, J. Zhang and X. Li, *ACS Appl. Mater. Interfaces*, **10**, 43031 (2018).
55. H. Zhang, R. Guo, J. Hou, Z. Wei and X. Li, *ACS Appl. Mater. Interfaces*, **8**, 29044 (2016).
56. M. Hou, W. Qi, L. Li, R. Xu, J. Xue, Y. Zhang, C. Song and T.

Wang, *J. Membr. Sci.*, **635**, 119541 (2021).
57. Y. Kim, W. Cho, Y. Kim, H. Cho and J. H. Kim, *J. Mater. Chem. C*, **6**, 8906 (2018).
58. Z. Tahir, M. Aslam, M. A. Gilani, M. R. Bilad, M. W. Anjum, L.-P. Zhu and A. L. Khan, *Sep. Purif. Technol.*, **224**, 524 (2019).
59. R. Patel, S. J. Kim, D. K. Roh and J. H. Kim, *Chem. Eng. J.*, **254**, 46 (2014).
60. S. Li, H. McGinness, T. Wang and R. Guo, *Polymer*, **237**, 124323 (2021).
61. S. Tachibana, K. Hashimoto, H. Mizuno, K. Ueno and M. Watanabe, *Polymer*, **241**, 124533 (2022).
62. S. Wang, Y. Xie, G. He, Q. Xin, J. Zhang, L. Yang, Y. Li, H. Wu, Y. Zhang, M. D. Guiver and Z. Jiang, *Angew. Chem. Int. Ed.*, **56**, 14246 (2017).
63. H. Dong, Z. Zhu, K. Li, Q. Li, W. Ji, B. He, J. Li and X. Ma, *J. Membr. Sci.*, **635**, 119440 (2021).
64. V. d. C. Cotlame-Salinas, A. López-Olvera, A. Islas-Jácome, E. González-Zamora and I. A. Ibarra, *React. Chem. Eng.*, **6**, 441 (2021).
65. J. M. Kolle, M. Fayaz and A. Sayari, *Chem. Rev.*, **121**, 7280 (2021).
66. X. Shi, H. Xiao, K. Kanamori, A. Yonezu, K. S. Lackner and X. Chen, *Joule*, **4**, 1823 (2020).
67. J. Faver and K. M. Merz, *J. Chem. Theory Comput.*, **6**, 548 (2010).
68. S. Pal and K. R. S. Chandrakumar, *J. Am. Chem. Soc.*, **122**, 4145 (2000).
69. Z. Dai, L. Bai, K. N. Hval, X. Zhang, S. Zhang and L. Deng, *Sci. China. Chem.*, **59**, 538 (2016).
70. L. Li, L. Huang, X. Lv, J. Wang, X. Li and Z. Wei, *Sep. Purif. Technol.*, **292** (2022).
71. J. Cheng, L. Hu, Y. Li, J. Liu, J. Zhou and K. Cen, *Appl. Surf. Sci.*, **410**, 206 (2017).
72. E. Ghasemi Estahbanati, M. Omidkhah and A. Ebadi Amooghin, *J. Ind. Eng. Chem.*, **51**, 77 (2017).
73. T. Khosravi and M. Omidkhah, *RSC Adv.*, **5**, 12849 (2015).
74. K. Shahrezaei, R. Abedini, M. Lashkarbolooki and A. Rahimpour, *Korean J. Chem. Eng.*, **36**, 2085 (2019).
75. M. Abdollahi, M. Khoshbin, H. Biazar and G. Khanbabaei, *Polymer*, **121**, 274 (2017).